

Low Energy X-ray Emission from Young Isolated Neutron Stars

M. RUDERMAN^{1,2,3}

¹*Department of Physics, Columbia University*

²*Columbia Astrophysics Laboratory, Columbia University*

³*Institute of Astronomy, Cambridge*

ABSTRACT. A young neutron star with large spin-down power is expected to be closely surrounded by an e^\pm pair plasma maintained by the conversion of γ -rays associated with the star's polar-cap and/or outer-gap accelerators. Cyclotron-resonance scattering by the e^- and e^+ within several radii of such neutron stars prevents direct observations of thermal X-rays from the stellar surface. Estimates are presented for the parameters of the Planck-like X-radiation which ultimately diffuses out through this region. Comparisons with observations, especially of apparent blackbody emission areas as a function of neutron star age, support the proposition that we are learning about a neutron star's magnetosphere rather than about its surface from observations of young neutron star thermal X-rays.

1. Introduction

A young, isolated, magnetized neutron star (NS) is expected to have several potentially important sources of low energy (\sim keV) X-ray emission (cf. Figure 1):

a) Thermal X-rays from the whole stellar surface as the NS cools down after a very high temperature birth in a supernova explosion.

b) Thermal X-rays from its much smaller but hotter polar caps, additionally heated by backflow to the stellar surface of extreme relativistic electrons or positrons. These leptons come from e^\pm producing accelerators on the open \mathbf{B} -field-line bundles which connect surface polar-caps to the spinning NS's distant "light-cylinder." These accelerators may be just above the NS surface ("polar-cap accelerators") or in the NS's outer-magnetosphere ("outer-gap accelerators").

c) Synchrotron radiation from newly created e^\pm pairs as the e^- and e^+ radiate away their initial momenta perpendicular to local \mathbf{B} .

The angular and spectral resolution achieved by the *Chandra* and *XMM* satellites allows discrimination of such NS radiation from that of the supernova remnant in which the youngest (age $t \lesssim 10^4$ yrs) NSs are usually embedded, and also thermal components (a and b) from the power law component (c); cf. Figure 2. In Section 2 we consider rather dramatic differences between observed thermal X-ray emission from young isolated hot neutron stars and the expected emission if the NS (near) magnetospheres were essentially empty. Section 3 discusses consequences for this emission if the NS magnetosphere within several NS radii of the stellar surface has an e^\pm pair density (n_\pm) large enough to give multiple cyclotron-resonance scattering of NS thermal X-rays before they ultimately escape or scatter back to the star. Section 4 estimates the steady state n_\pm and its consequences for observed NS thermal spectra. Section 5 summarizes some conclusions and further problems.

2. Observations and models

Reported thermal X-ray luminosities (L_X^T) of young isolated neutron stars are shown as a function of NS "age" (t) in Figure 3. (The "age" is generally that of the SNE envelope around the NS when that can be estimated. For some of the youngest NSs, J2323, J0852, J1617, and J0821 spin-period P with spin-down-rate \dot{P} are not known so

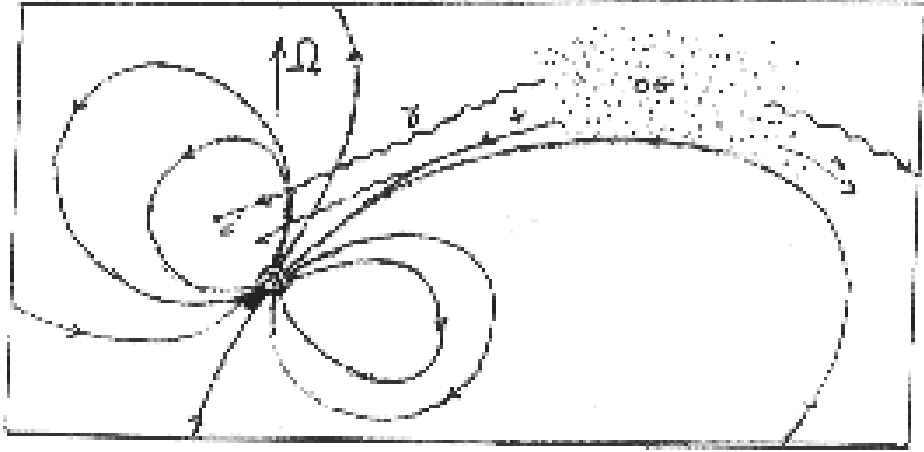


Fig. 1. An outer-gap (OG) accelerator, extending along the open field line bundle on both sides of its intersection with the null-surface where $\Omega \cdot \mathbf{B} = 0$. GeV γ -rays directly from this accelerator may produce e^\pm pairs close to the neutron star. 10^2 MeV γ -rays, curvature radiated by TeV $e^+(e^-)$ flowing out of this accelerator down to the star, will be a very strong source for such e^\pm . On the other side of the star a polar cap (pc) accelerator may also be a strong source for $\gamma \rightarrow e^+ + e^-$. (Because e^\pm pairs from OG accelerators can quench PC accelerators and vice versa, it is unlikely that a particular bundle of open field-lines would sustain both.)

the canonical spin-down age ($P/2\dot{P}$) cannot be used.) The computed thermal L_X^T is that for the simplest, initially very hot, $1.4M_\odot$ neutron star model: a core consisting solely of neutrons, protons and extreme relativistic electrons, surrounded by a relatively thin more poorly conducting crust which keeps the NS surface temperature (T) very much less than that at the crust-core boundary (T_c). Although model T depends upon assumed NS surface detail, L_X^T from core-cooling should not as long as $T_c \gg T$. Disagreement between model estimates and observations is not great, and usually compatible with uncertainties in the distance to the NS. (PSR 1055, for example, may well be half as far away as the value used in Figure 3, decreasing its L_X^T by a factor four. Some of the extremely young NSs may have apparent L_X^T which are strongly diminished when they are observed along particular lines-of-sight, as discussed in Section 5e.) Comparison between predictions and observations of Figure 3 do not discourage attribution of those L_X^T to the expected NS cooling.

However, there are two great surprises in the observed thermal spectra of the NSs.

1) None of the spectral features calculated for NS surface compositions other than H (and, presumably, He) are observed (with the remarkable exception of 1E1207 which may have a very different explanation to be discussed elsewhere). Indeed, a blackbody spectrum is generally an acceptable fit to observations and radiation parameters (surface temperature and radiating area) have usually been calculated for it.

2) The effective blackbody radiating area (A_{BB}) has the magnitude and age dependence indicated in Figure 4, hugely different from a simple age independent $A_{BB} \sim A_{NS} \equiv 4\pi(R_{NS})^2 \sim 4\pi(10 \text{ km})^2 \sim 10^{13} \text{ cm}^2$. Instead, observations give

$$\frac{A_{BB}}{A_{NS}} \sim 3 \cdot 10^{-2} \left(\frac{t}{10^4 \text{ yrs}} \right) \quad (1)$$

for $t \lesssim 10^5$ yrs; and $A_{BB}/A_{NS} \sim 0(1)$ only for older NSs. If, despite the support of Figure 3 for the observed L_X^T being mainly powered by core cooling, it is assumed

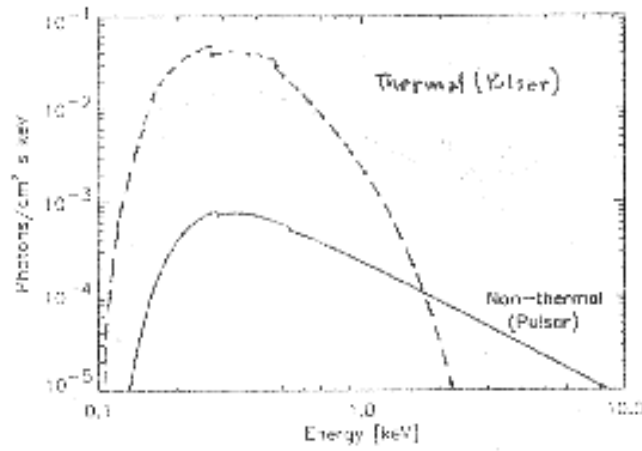


Fig. 2. X-ray count flux from the Vela pulsar (after removal of nebular emission). (After Mori et al. 2002.)

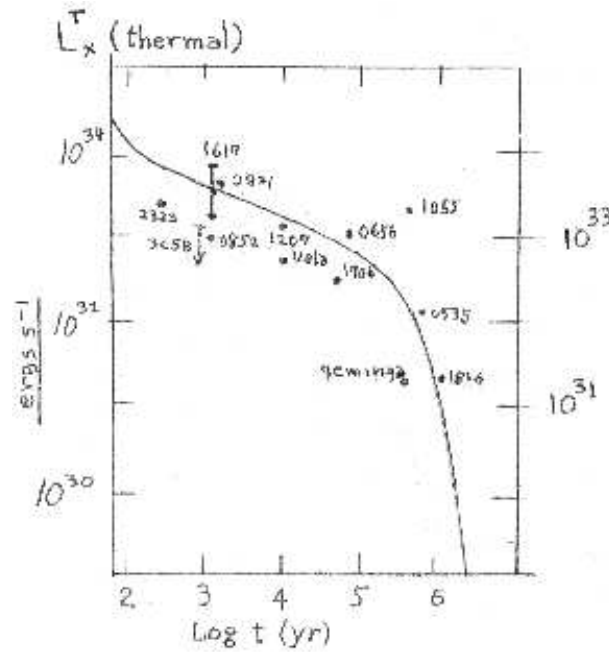


Fig. 3. Thermal X-ray luminosity (L_X^T) of young isolated canonically magnetized neutron stars as a function of stellar age (t). Observed L_X^T are from summaries of *XMM* and *Chandra* results (Becker & Aschenbach 2002; Pavlov et al. 2002) supplemented with data from Gotthelf et al. (2002) for PSR B1706, McGowan et al. (2003) for J0538, Mori et al. (2002) for Vela, and Wang & Halpern (1997) for Geminga. The solid line model curve for L_X^T to which these data are compared is based upon Page (1998); cf. Tsuruta (1997).

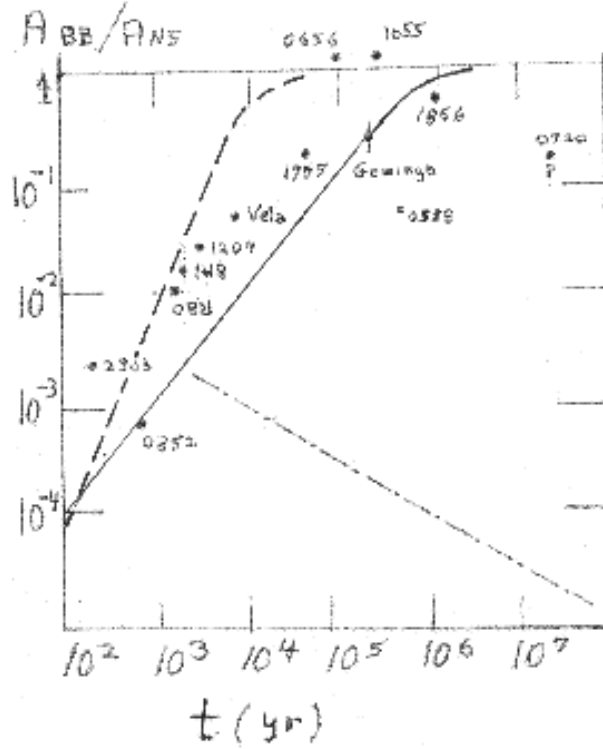


Fig. 4. Blackbody fits for thermal radiation areas of isolated neutron stars (A_{BB}), in units of a nominal neutron star surface area $A_{NS} = 4\pi(10\text{km})^2$, as a function of neutron star age. (References for these data are the same as those for Figure 3.) The decreasing dash-dot diagonal is the model area of a hot polar cap of a central dipole. The upper dashed line is from the $\tau = 10^{-3}\text{s}$ e^\pm outflow model of Section 4; the lower solid line is from the $\tau = 0\text{s}$ model in which e^\pm flow before $e^+ + e^- \rightarrow \gamma + \gamma$ annihilation is assumed to be ignorable.

that the dominant sources of L_X^T are the hotter polar caps, the difference between expectations and observed black body areas becomes even greater: NSs with central dipoles (or uniform interior magnetization) have polar caps of area (A_{pc}) with

$$\frac{A_{pc}}{A_{NS}} \sim \frac{5 \cdot 10^{-5}}{P(\text{sec})}. \quad (2)$$

This ratio is shown as the downward sloping dashed line of Figure 4, differing even more dramatically in both slope and magnitude from observations than does $A_{BB}/A_{NS} \sim 1$.

If it is assumed that the NS surface, instead being a perfect absorber, has an H-atmosphere, L_X^T is not much changed. The associated affective radiating areas for near keV X-rays still grow almost linearly with t but now would have very significantly greater magnitudes. Typically the two different inferred NS surface temperatures, T_{BB} and T_H , differ by about a factor two; $T_{BB} = (1.5-3)T_H$ (Pavlov et al. 2002; Becker & Aschenbach 2002) and have area ratios inversely proportional to the surface T^4 . Then for putative H-atmospheres when only blackbody parameters have so far been reported it seems plausible to estimate $A_H \sim 2^4 A_{BB}$: the youngest NSs would still have $A_H/A_{NS} \ll 1$. The dramatic rise and subsequent leveling off in radiating areas would still remain and require explanation.

3. Thermal X-rays observed from a hot strongly magnetized neutron star embedded in a dense e^\pm plasma

A surrounding e^\pm plasma with number density $n_\pm = n_+ = n_- < 10^{17} \text{cm}^{-3}$, extending out to several stellar radii around a NS, would not give important Thomson cross section scattering of thermal X-rays emitted from the NS surface. However, because the thermal X-ray's energy ($E_X = \hbar\omega \sim \text{keV}$) is less than the e^- and e^+ cyclotron-resonance energy at the stellar surface ($\hbar\omega_B = eB\hbar/mc \sim 10B_{12}\text{keV}$), an emitted thermal X-ray will pass through a cyclotron-resonance where $E_X - \hbar\omega_B(r)$ within a few stellar radii of the emitting surface (Wang et al. 1998, Zhu & Ruderman 1997, Dermer & Sterner 1991, Mitrofanov & Pavlov 1982). The resonant polarization-averaged X-ray scattering cross section there is well approximated as

$$\sigma_\pm \sim \frac{4\pi^2 e^2}{mc} \delta[\omega - \omega_B(r)]. \quad (3)$$

We assume below that equation (3) also adequately approximates the scattering cross section for any polarized x-ray if the averaging is over its e^- and e^+ scattering cross sections. (This fails when the photon's momentum is almost perpendicular to local \mathbf{B} together with its electric polarization being almost parallel to \mathbf{B} . However, when the optical depth for such resonance scattering is very large, as in the main applications discussed below, or the near-star \mathbf{B} -field is very irregular, the limit to accuracy from the use of Equation 3 does not substantively alter the conclusions which will be based upon it.)

With the σ of Equation 3, the optical depth for cyclotron-resonance scattering (OD) of an energy E_X X-ray is about $(\lambda_X / \frac{e^2}{mc^2}) \sim 10^5$ times that for non-resonant Thomson scattering:

$$OD = \int_{R_{NS}}^{\infty} \sigma_\pm n_\pm dr \sim \frac{4\pi^2 e^2 r_B \hbar n_\pm}{3mcE_X} \quad (4)$$

as long as r_B , the distance from the NS center where $\hbar\omega_B = E_X$, satisfies $r_B > R_{NS}$. (The denominator factor 3 is based on B -field r -dependence of a central dipole.)

The cyclotron-resonance backscatter radius $r_B \sim 3R_{NS}$ for an $E_X \sim 1\text{keV}$ X-ray emitted from a NS with surface dipole field $3 \cdot 10^{12}\text{G}$. This backscattering region around $r \sim 3R_{NS}$ forms a reflecting, slightly leaky *Hohlraum* container holding in radiation from the NS. Its X-ray transmission coefficient

$$\hat{t} \sim \left(\frac{2}{2 + OD} \right), \quad (5)$$

and the container X-ray reflection coefficient $\hat{r} = 1 - \hat{t} \sim OD(OD + 2)^{-1}$. When $\hat{t} \ll R_{NS}^2/r_B^2 \sim 10^{-1}$, an X-ray emitted from the NS surface will almost always be reflected by the *Hohlraum* container and then reabsorbed by the NS before escaping the *Hohlraum*. In this regime the *Hohlraum*-contained X-rays acquire a Planck-blackbody energy spectrum independent of the NS surface's emission and reflection properties. It is sensitive only to the (now higher) surface temperature of the NS.

In a steady state the total outflow luminosity is unchanged by the e^\pm plasma in which the NS is embedded. Equivalently, the container has a surface emissivity $\hat{e} \approx \hat{t} = 1 - \hat{r}$ and

$$L_X \equiv A_{BB} \sigma_{SB} T_{BB}^4 = 4\pi r_B^2 \hat{e} \sigma_{SB} T_{BB}^4 \quad (6)$$

(with σ_{SB} the Stefan Boltzmann constant).

Then from Equations (5) and (6)

$$A_{BB} \simeq \hat{e} 4\pi r_B^2 \simeq \frac{8\pi r_B^2}{OD} \quad (7)$$

as long as the computed R_{NS} of Equation (7) gives an $A_{BB} \ll 4\pi R_{NS}^2$. In the opposite limit, as OD drops below $(r_B/R_{NS})^2/2$, $A_{BB} \rightarrow 4\pi R_{NS}^2$. If A_{BB} varies greatly with E_X observed emission out from the *Hohlraum*'s container would have a spectral distribution significantly different from the interior Planck one.

4. Inferred radiation areas (A_{BB}) and neutron star spin-down age

In a steady state the production rate of e^\pm pairs near a spinning-down NS (\dot{N}_\pm) needed to maintain a constant local pair density n_\pm in the relevant cyclotron-resonance scattering region is balanced by the sum of two local pair removal rates:

a) Local annihilation into γ -rays (\dot{n}_\pm^a) with

$$n_\pm^a \sim 2\pi \left(\frac{e^2}{mc^2} \right)^2 c (n_\pm)^2; \quad (8)$$

(assuming nonrelativistic $e^+ - e^-$ relative velocities along \mathbf{B} and anti-parallel magnetic moments along the strong local \mathbf{B} have been achieved).

b) Pair outflow (\dot{n}_\pm^f) from strong push of incident thermal X-rays on the continually replenished cyclotron-resonant container of the *Hohlraum* give a finite residence time (τ) there:

$$\dot{n}_\pm^f \sim -\frac{n_\pm}{\tau}. \quad (9)$$

One estimate for the τ follows from the assumption that very quickly after the pair creation the e^\pm speed along local \mathbf{B} becomes such that the push on $e^- + e^+$ is perpendicular to local \mathbf{B} (about 10^{10} cm s $^{-1}$). Then to move along that \mathbf{B} through the container thickness ($\sim r_B \sim 3R_{NS} \sim 3 \cdot 10^6$ cm) takes

$$\tau \sim 10^{-3} \text{s}. \quad (10a)$$

[Pair inflow from NS gravitational pull could be important if that pull were greater than the outward push by contained *Hohlraum* X-rays. In the models presented here the pressure for that outward push is about $(OD/2)(L_X^T/4\pi r_B^2 c)$. The oppositely directed pull from the weight of the n_\pm around r_B which constitute the container (Equation 4) is only $10^{-3}(10^{33} \text{erg s}^{-1}/L_X^T)$ as large. Therefore we do not consider it further here. This interpretation does not support the gravity dependent e^\pm -layer structure and X-ray spectra proposed for the Crab pulsar by Zhu and Ruderman (1997); cf. also Wang et al. (1998).]

At the other extreme, if this local \mathbf{B} near the NS is still so ‘‘complicated’’ that e^\pm is kept from flowing out before annihilation,

$$\tau \sim \infty. \quad (10b)$$

The near-star pair input rate may be even more difficult to estimate than the annihilation rate. Pairs on closed field lines very near a young NS ($r \lesssim 3R_{NS}$) can be created by a) MeV - GeV γ -rays which enter into that region from outer-gap accelerators; b) MeV - 10^2 MeV curvature γ -rays from TeV $e^+(e^-)$ flowing down to a NS polar cap on \mathbf{B} -field lines connecting the polar cap to the outer-gap accelerators; and c) 1 - 10^2 MeV γ -rays generated by polar cap accelerators on open-field lines, and then bent over to cross near-surface closed-field lines by the strong NS gravitational pull on them (a source which becomes large and important when the usual central dipole model for \mathbf{B} is replaced by a more realistic one without axial symmetry).

A further complication in calculating \dot{N}_\pm near the NS is a possible second generation of e^\pm production by GeV γ -rays from outer-gap accelerators. The e^\pm pairs they create, if

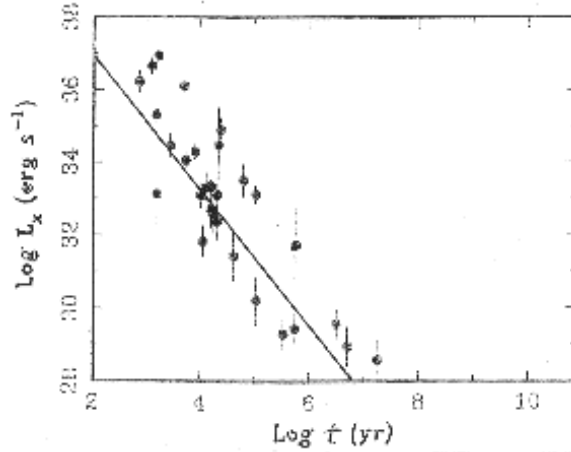


Fig. 5. X-ray luminosity (L_X) for $2 \text{ keV} < E_X < 10 \text{ keV}$ of canonically magnetized isolated neutron stars as a function of their ages (Possenti et al. 2002). The solid curve is Equation 12: $L_C = 10^{33} (10^4 \text{ yrs}/t)^2 \text{ erg s}^{-1}$.

these γ -rays pass are within $10R_{NS}$ of the NS, can themselves be the source of energetic ($E_\gamma > 1 \text{ MeV}$) synchrotron γ -rays. These, in turn, would create more pairs if they pass into the much stronger \mathbf{B} much closer to the star (Cheng & Zhang 1999; Chang et al. 1998; Yakovlev et al. 2002). A rough estimate for the Vela pulsar suggests that $\dot{N}_\pm \sim 10^{37} - 10^{38} \text{ s}^{-1}$ for this pulsar.

A more empirical, and probably more reliable, estimate of \dot{N}_\pm near the NS comes from identifying the Vela power law component of Figure 1 with the x-ray synchrotron radiation from the immediate quenching of e^- and e^+ perpendicular momenta of all newly created e^\pm pairs in the strong local \mathbf{B} (Wang et al. 1998). The power law synchrotron luminosity from the local field where the e^\pm are created by $\sim 10^2 \text{ MeV}$ γ -rays has a total power law luminosity (L_X^{PL}) for $2 \text{ keV} < E_X < 10 \text{ keV}$

$$L_x^{PL}(2 - 10 \text{ keV}) \sim \dot{N}_\pm mc^2 \left(\frac{8 \text{ keV}}{\hbar \omega_B} \right)^{1/2} \sim 10^{-5} \dot{N}_\pm \text{ erg s}^{-1}, \quad (11)$$

where the local \mathbf{B} field is assumed to be around 10^{10} G so that $\hbar \omega_B \sim 10^{-1} \text{ keV}$. If the L_X^{PL} is indeed from such synchrotron radiation, its X-ray photon flux spectrum between 2 and 10 keV should be $\sim E_X^{-\Gamma}$ with $\Gamma \sim 1.5$ as long as all relevant $\hbar \omega_B \lesssim 2 \text{ keV}$ and maximum synchrotron radiation energy $E_X > 10 \text{ keV}$. [Although reported Γ ranges do not always include this value it is compatible with many examples: 1.25 – 1.45 for Vela, 1.4 – 1.5 for PSR 0656, 1.6 for the Crab (Becker & Aschenbach 2002) and 1.66 for PSR 1055 (Pavlov et al. (2002).]

Observed (2 – 10 keV) L_X as a function of NS ages are shown in Figure 5. (In this range for E_X , L_X is expected to be dominated by its power law component.)

We approximate a fit to these data by the line shown there:

$$L_X^{PL} \sim L_X = 10^{33} \left(\frac{10^4 \text{ yrs}}{t} \right)^2 \text{ erg s}^{-1}. \quad (12)$$

When combined it with the defining relations $B_d^2 \equiv R^{-6} c^3 \Omega^{-4} \times$ (spin-down power $|I\Omega\dot{\Omega}|$) and NS spin-down age $t = -\Omega/2\dot{\Omega}$, Equation 12 becomes $L_X \sim 4B_d^2 R_{NS}^6 I^{-2} \times |$

spin-down power|. For canonical pulsars with $B_d \sim 10^{12}$ G it is then roughly equivalent to the empirical Becker-Trümper relation (Becker & Trümper 1997; Seward & Wang 1998; Possenti et al. 2002.) $L_X \sim 10^{-3}$ |spin-down power|.

To calculate the needed n_{\pm} by combining the total pair creation rate \dot{N}_{\pm} from Equations 11 and 12 with the local disappearance rates of Equation (8, 9 and 10), it is necessary to estimate the volume (V_{\pm}) in which the pair creation rate of \dot{N}_{\pm} is achieved. This depends upon the characteristic \mathbf{B} in which the $\gamma + \mathbf{B} \rightarrow e^{\pm} + \mathbf{B}$ occurs, the same \mathbf{B} as that of ω_B in Equation 11. For that $\hbar\omega_B \sim 10^{-1}$ keV, corresponding to e^{\pm} production beginning at $B \sim 10^{10}$ G by characteristic 10^2 MeV curvature γ -rays from the TeV e^{-} (e^{+}) flow outward from a polar-cap accelerator and inward from an outer-gap one,

$$V_{\pm}(\propto \omega_B^{-3}) \sim 10^{21}\text{cm}^3. \quad (13)$$

Combining Equations 7 and 4 with $r_B = 3 \cdot 10^6$ cm and $E_X = 1$ keV, together with Equations 8, 9, 11, 12, and 13, gives n_{\pm} , OD , and the two A_{BB}/A_{NS} model curves shown in Figure 4. To obtain the solid curve we pretend that equation 10b is the appropriate entry for Equation 9, i.e., a very complex closed B-field structure to $r \sim r_B$. The opposite $\tau = 10^{-3}$ s approximation of Equation 10a gives the upper dotted line. The truth may well lie somewhere between the curves shown.

5. Some conclusions, speculations, and problems

The model results for estimated A_{BB} magnitudes and their age dependence are qualitatively similar to the observed ones of Figure 4 over several orders of magnitude. This gives considerable support to our central proposition. Strongly magnetized NSSs with large spin-down powers continually produce enough e^{\pm} pairs on the closed B-field lines in their strongly magnetized near-magnetospheres that X-ray cyclotron-resonant scattering there preempts direct observation of the NS surface.

Although comparisons between these over-simplified models and NS thermal X-ray observations may not be quantitatively reliable they encourage further model-based interpretations of existing thermal X-ray observations.

If the $\tau = 10^{-3}$ s model (uppermost curve) in Figure 4 leads to a reasonable approximation for e^{\pm} cyclotron-resonance opacity around a young neutron star, that opacity alone would not explain why the NSs older than 10^4 yrs would have L_X^t fits to near blackbody spectra and A_{BB}/A_{NS} so much less than unity. These two features suggest that for those NSs (but not for younger ones) it may be more appropriate to fit observed thermal spectra with unobstructed emission from H or He atmospheres. (This seems, however, often to give optimal fits with A_H/A_{NS} enough larger than unity to introduce new problems.)

If the $\tau \rightarrow \infty$ model is a better description, surrounding e^{\pm} plasma blackbody-like emission from a slightly leaky e^{\pm} *Hohlraum* container would remain appropriate for very considerably older NSs (lower curves of Figure 4). However, at least one of these, J0538, would be expected to have such small surrounding e^{\pm} opacity that the observations still suggest its interpretation as a NS emitting unobstructed thermal X-rays from an H (or He)-atmosphere with

$$\frac{A_H}{A_{NS}} \sim \left(\frac{T_{BB}}{T_H} \right)^4 \frac{A_{BB}}{A_{NS}} \sim 2^4 \frac{A_{BB}}{A_{NS}} \sim 1. \quad (14)$$

A more accurate description of the large n_{\pm} around very young magnetized spinning-down NSs will be needed for many observational details.

a) Variation of n_{\pm} and thus OD , with (angular) location. This would give spin-phase modulation to the observed thermal flux.

b) The dependence of r_B^2/OD on X-ray frequency, causing some departure from a Planck spectrum in emission. (If the \dot{N}_\pm which sustains n_\pm is inside r_B and n_\pm outflow through relevant r_B conserves $r\pi r^2 n_\pm$. Equation 4 does give $r\pi r_B^2/OD$ independent of X-ray energy when $B \propto r^{-3}$.) Another neglected departure of thermal X-ray emission from exact Planck spectra comes from significant e^+/e^- flow velocities along \mathbf{B} : e^+/e^- recoil is very small in each cyclotron-resonance X-ray scatter ($E_X/mc^2 \ll 1$) but not X-ray energy boost or degradation.

c) Inclusion of backscatter of hotter polar-cap X-rays which suppresses discrimination between the separate contributions to L_X of polar cap emission and general surface cooling.

d) Correlations among L_X^{PL} , A_{BB} , and dipole moment for individual NSs. For example, special consideration must be given to relating \dot{N}_\pm to L_X^{PL} from pulsars with exceptionally large B ($\sim 10^6$ G) near their light cylinders. When such pulsars have strong outer-gap accelerators in that region, GeV (curvature) γ -rays + keV X-rays produce pairs there with very strong initial synchrotron radiation in the 2 – 10 keV range. For these e^\pm , local $\hbar\omega_B \sim 10^{-2}$ eV so Equation 11 becomes $\dot{N}_\pm \sim 10^3 L_X^{PL}$ (erg s^{-1}) instead of the much larger inferred \dot{N}_\pm from L_X^{PL} if the e^\pm pairs are produced very near the NS. This distinction should be important for the Crab pulsar with its exceptionally large light-cylinder B ($\sim 10^6$ G). The Crab pulsar's observed L_X^{PL} (2 – 10 keV), $\sim 10^{36}$ erg s^{-1} , should and does lie well above the $L \propto t^{-2}$ line in Figure 5. Its L_X^{PL} should not be used without adjustment to predict \dot{N}_\pm in the Crab pulsar magnetosphere and especially not in the inner-magnetosphere near the star. (A total crab pulsar \dot{N}_\pm inferred from Equation 11, without taking into account its large expected outer-magnetosphere contribution to L_X^{PL} , would exceed observational upper limits for the Crab pulsar's half MeV annihilation γ -rays from $e^+ + e^- \rightarrow \gamma + \gamma$, $(0.5 - 1) \times 10^{40} \text{s}^{-1}$ (Ulmer et al. 2001; Massaro et al. 1991; Zhu & Ruderman 1997).

e) Differences between total L_X^T and that inferred from observations because the spin cycle averaged OD may vary greatly for observers along different lines-of-sight to the NS center. In particular, there is the possible escape of *Hohlraum* X-rays through an open field-line bundle “hole” (area $\sim \pi r_B^3 \Omega c^{-1}$) in the *Hohlraum* container. (Because of the large very relativistic particle flow in the bundle sustained by the accelerator somewhere on it, OD along it can be greatly suppressed at $r \sim r_B$ for thermal x-ray frequencies. Then, for pulsars with relatively large “hole” areas and large n_\pm elsewhere, *Hohlraum* X-rays may mainly pass out through the container's polar-cap-like “holes” rather than diffuse out through the container's reflecting “wall”. When this obtains, the concentration of L_X^T outflow through such holes could increase its apparent value by about a factor 2, or decrease it by a very much greater factor, depending on polar cap locations and that of the line-of-sight to the observer. (The rapidly spinning NS in 3C58 (J0205 with $P = 66$ ms) with very large spin-down power ($2 \times 10^{37} \text{erg s}^{-1}$) would be expected to have a very large \dot{N}_\pm and thus n_\pm . X-ray outflow through container holes should be greater than the diffusive one. To an observer for whom the container holes are largely hidden during the full NS spin cycle most of that NS's L_X^T could be directed away from the observer. If so, the inferred L_X^T magnitude would be greatly reduced from its true value. This may well account for not yet observing any L_X^T from it (cf. Slane et al. 2002).

Effects of \dot{N}_\pm may be complicated and difficult to evaluate quantitatively but their consequences may be crucial for interpreting observations of low energy X-ray fluxes from young isolated neutron stars.

Acknowledgements

I am pleased to thank many colleagues for patient listening and informing, especially W. Becker, E. Gotthelf, C. Hailey, J. Halpern, D. Helfand, C. Ho, K. Mori, F. Paerels, G. Pavlov, M. Rees, J. Trümper, and M. Weisskopf.

References

- Becker, W., Trümper, J.: 1997, *Astron. Astrophys.* **326**, 682.
- Becker, W., Aschenbach, B.: 2002, Proc. 270 WE-Heraeus Seminar “Neutron Stars, Pulsars and Supernova Remnants,” eds. W. Becker, H. Lesch, J. Trümper, MPE Rpt. 278, astro-ph/0208466.
- Cheng, K., Zhang, L.: 1999, *Astrophys. J.* **515**, 337.
- Cheng, K., Zhang, L.: 1998, *Astrophys. J. Lett.* **493**, L35.
- Dermer, C., Sturmer, S.: 1991, *Astrophys. J. Lett.* **467**, L23.
- Eilek, J., Arendt, P., Hankins, T., Weatherall, J.: 2002, Proc. 270 WE-Heraeus Seminar “Neutron Stars, Pulsars and Supernova Remnants,” eds. W. Becker, H. Lesch, J. Trümper, MPE Rpt. 278.
- Gotthelf, E., Halpern, J., Dodson, R.: 2002, *Astrophys. J. Lett.* **567**, L125.
- McGowan, K., Kennea, J., Zane, S., Cordova, F., Cropper, M., Ho, C., Sasseen, T., Vestrand, W.: 2003, *Astrophys. J.* **591**, 380.
- Mori, K., Hailey, C., Paerels, F., Zane, S.: 2002: Cospar Proceedings.
- Possenti, A., Cerutti, R., Colpi, M., Mereghetti, S.: 2002, *Astron. Astrophys.* **387**, 993.
- Mitrofanov, I., Pavlov, G.: 1982, *Mon. Not. R. Astr. Soc.* **200**, 1033.
- Massaro, E. et al.: 1991, *Astrophys. J. Lett.* **376**, L11.
- Page, D.: 1998, in The Many Faces of Neutron Stars, NATO ASI Ser. C., vol 515 p. 538. ed. R. Buccheri, J. van Paradijs, M. Alpar (Kluwer, Dordrecht).
- Pavlov, G., Zalin, V., Sanwal, D.: 2002, Proc. 270 WE-Heraeus Seminar “Neutron Stars, Pulsars and Supernova Remnants,” eds. W. Becker, H. Lesch, J. Trümper, MPE Rpt. 278, astro-ph/0206024.
- Seward, F., Wang, Z.: 1998, *Astrophys. J.* **332**, 199.
- Slane, P., Helfand, D., Murray, S. 2002, APJL 571 45.
- Tsuruta, S.: 1997, *Physics Reports*, **290**, 3.
- Ulmer, M., Matz, S., Grove, J., Strickman, M., Kurfess, J., Ruderman, M., Zhu, T., Ho, C.: 2001, *Astrophys. J.* **551**, 244.
- Wang, F., Ruderman, M., Halpern, J., Zhu, T.: 1998, *Astrophys. J.* **448**, 373.
- Wang, F., Halpern, J.: 1997, *Astrophys. J. Lett.* **482**, L159.
- Yakovlev, D., Gnedin, O., Kaminker, A., Potekhin, A.: 2002, Proc. 270 WE-Heraeus Seminar “Neutron Stars, Pulsars and Supernova Remnants,” eds. W. Becker, H. Lesch, J. Trümper, MPE Rpt. 278.
- Zhu, T., Ruderman, M.: 1997, *Astrophys. J.* **478**, 701.